HETEROCYCLES, Vol. 104, No. 3, 2022, pp. 447 - 469. © 2022 The Japan Institute of Heterocyclic Chemistry
Received, 25th October, 2021, Accepted, 1st December, 2021, Published online, 2nd December, 2021
DOI: 10.3987/COM-21-14578

NOVEL PYRAZOLINES AND BENZOTHIAZEPINES AS TUBULIN POLYMERIZATION INHIBITORS: SYNTHESIS, BIOLOGICAL EVALUATION, AND MOLECULAR DOCKING

Alaadin E. Sarhan,[a]* Ashraf A. Sediek,[b] Nagy M. Khalifa,[c] and Essam E. Hasan[d]

[a,c] Therapeutic Chemistry Department, Pharmaceutical and Drug Industries Institute, National Research Centre, Dokki, Cairo, 12622 Egypt.
E-mail: dralaasarhan1968@outlook.com
[b] Chemical Industries Institute, National Research Centre, Dokki, Cairo, 12622 Egypt
[d] Drug Bioavailability Centre, National Organization for Drug Control and Research (NODCAR), Giza, Egypt

Abstract – Synthesis, biological evaluation, and molecular docking of pyrazoline-linked benzenesulfonamides and diaryl 1,5-benzothiazepines prepared from new chalcones are described and elucidated. Novel compounds were studied for their *in vitro* anticancer profiles on HepG2, HEK-293, MCF-7, and MDA-MB-231 cancer cell lines, where, compounds **IIb**, **III**, and **IVe** demonstrated high to moderate cell proliferation inhibition activity. Compound **IIb** was further assessed for tubulin polymerization inhibition effects due to its high potency, which showed superior suppression compared to the reference drug. It induced cell cycle cessation at the G2/M phase and accumulation of cells in the pre-G1 phase, preventing its mitotic cycle. In addition, compound **IIb** activated caspase-7, mediating apoptosis of HepG2 cells. These findings, along with molecular docking and pharmacophore constructed models, provide a new scaffold of cytotoxic agents targeting tubulin.

INTRODUCTION

For decades, scientists have attempted to look for specific inhibitors of key nods in cancer pathways, and their great efforts have led to positive feedback with many approved drugs. Recent drug discovery has sparked interest in allosteric site inhibitors or agonists with synergistic effects.[1,2] However, chimeric

antigen receptor T-cell immunotherapy (CAR-T) and programmed cell death protein 1 (PD-1) appear to be the hottest spots in this field right now.[3] Given the negative impact of both strategies, many researchers have focused on similar synergistic strategies, one of which is tubulin-related functional molecules,[4] which can cause remarkable variation in microtubule dynamics, thereby regulating the mitotic catastrophe process.[5] The microtubule had four distinct binding sites: a site for microtubule stabilizer, which includes the taxane site and the laulimalide/peloruside along with the vinca site and the colchicine site for microtubule destabilizer.[6,7] However, colchicine has received the most attention because of the low level of multidrug resistance and its binding site has the potential to be used to deliver anti-cancer agents.[8] Furthermore, unlike other cell death processes that are induced by a variety of agents at high doses, mitotic catastrophe can be initiated by cytotoxic agents at low doses,[9] where colchicine and vinblastine were typical agents[10] suggesting a potential therapeutic cut-in point.

It was reported that compounds **A-C** targeting the colchicine site to regulate the mitotic process were going to the clinical trial stage (Figure 1).[11-13] In addition, promising compounds **D-F** were synthesised to inhibit tubuline polymerization (Figure 2).[14-16]

As a part of our research on bioactive heterocyclic and pharmaceutical compounds,[17-21] in this work, we developed anti-tubulin agents, based on chalcones as important precursors with novel backbone compounds for the synthesis of a variety of heterocyclic compounds using benzothiazepine and pyrazoline rings to act as linkers between essential rings based upon reported structures, in a trial to test a new ideas in both structural evolution and therapeutic approaches.

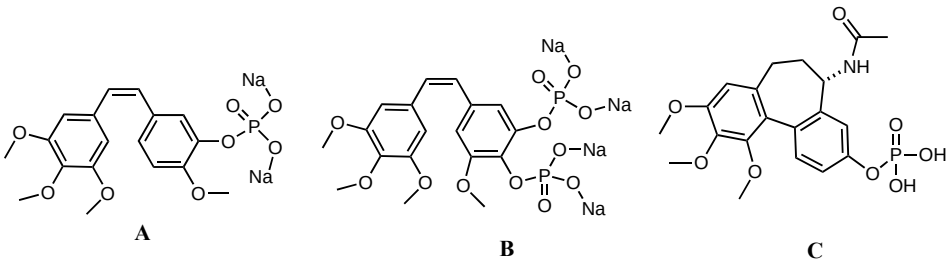

Figure 1. Inhibitors targeting tubulin at colchicine site

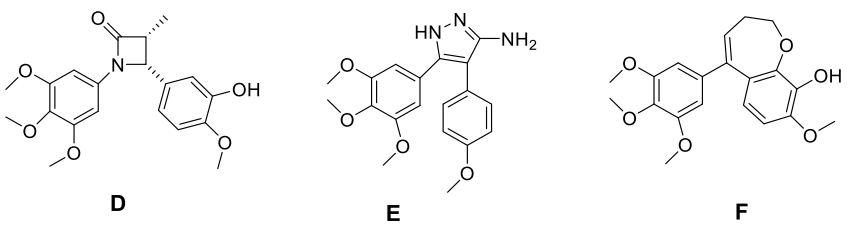

Figure 2. Tubulin polymerization inhibitors-linker-modifications

RESULTS AND DISCUSSION

Chemistry

The synthetic procedures to obtain the target products were initiated by the Claisen-Schmidt condensation reaction of different substituted acetophenones with 4-(3-hydroxypropoxy)-3-methoxybenzaldehyde in basic medium to yield the desired chalcones **Ia-e** (Scheme 1). The IR spectra revealed the existence of C=O function conjugated with the olefin bond CH=CH, which appeared at a lower wave number in the range of 1658-1651 cm^{-1}. The formation of the CH=CH–CO group was also confirmed by the appearance of two doublet signals at δ = 7.78-7.89 ppm and δ = 7.38-7.74 ppm with a coupling constant of 15.5 Hz confirmed the trans configuration. ^{13}C NMR spectra showed the presence of a carbonyl group at δ = 189.17-189.90 ppm along with the olefin carbons around δ = 143.27-145.12 and δ = 121.60-123.18 ppm.

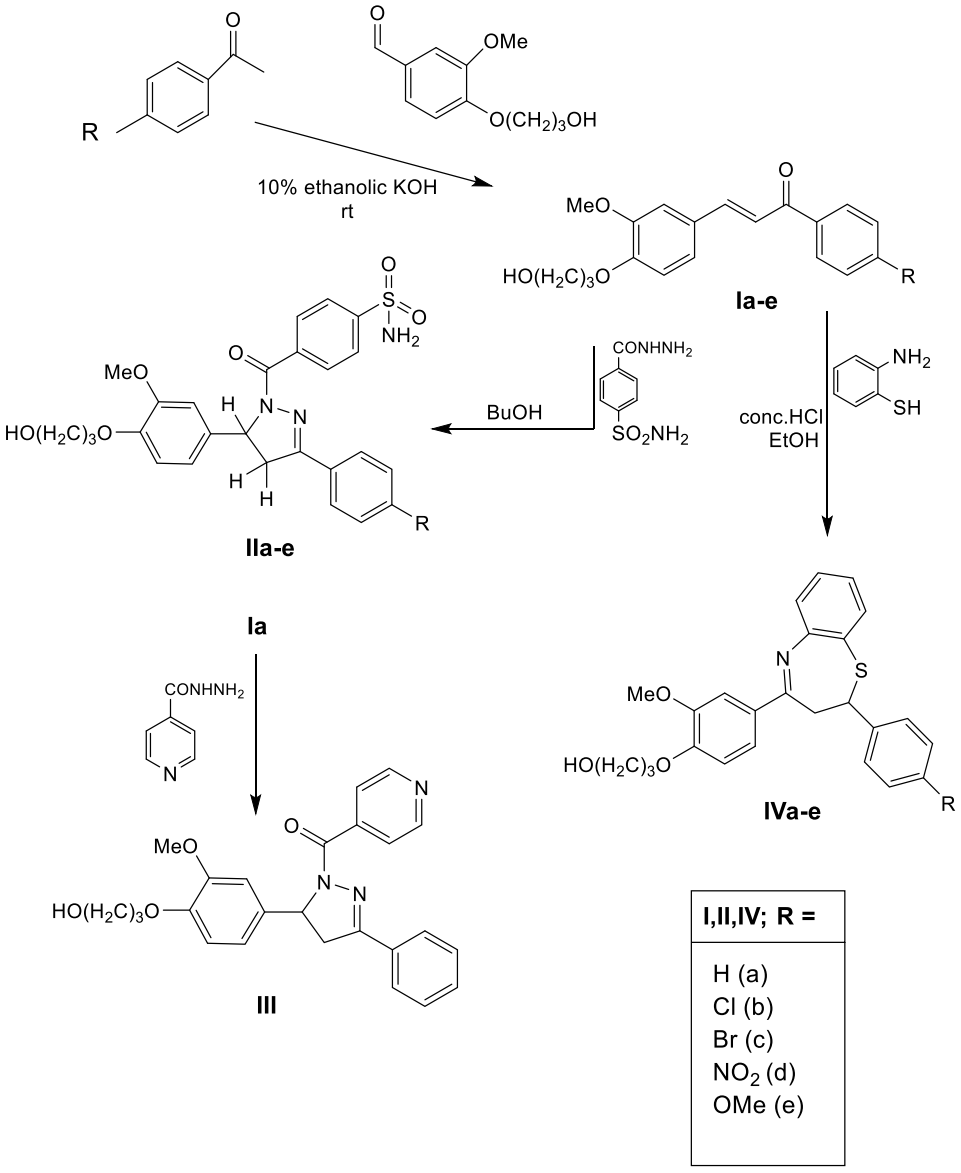

Scheme 1. Synthesis of pyrazoline-linked benzenesulfonamides and other derivatives

Treatment of chalcone derivatives **Ia-e** with 4-(hydrazinecarbonyl)benzenesulfonamide in refluxing butanol gave the target pyrazolines **IIa-e** *via* two kinds of additions: 1,2- and Michael additions (Scheme 2).[22] The formation of pyrazoline moiety in the resulted products was confirmed by ^{1}H NMR spectrum, in which methylene proton resonated as a pair of doublets observed at δ = 3.13-3.46 ppm and δ = 3.66-3.99 ppm. The C-H proton appeared as a doublet of doublets at δ = 5.42-5.89 ppm due to the vicinal coupling with the magnetically non-equivalents proton of the methylene. Further, in ^{13}C NMR spectra of **IIa-e**, C-4 and C-5 of the pyrazoline nucleus appeared around δ = 43.0 and δ = 62.0 ppm.

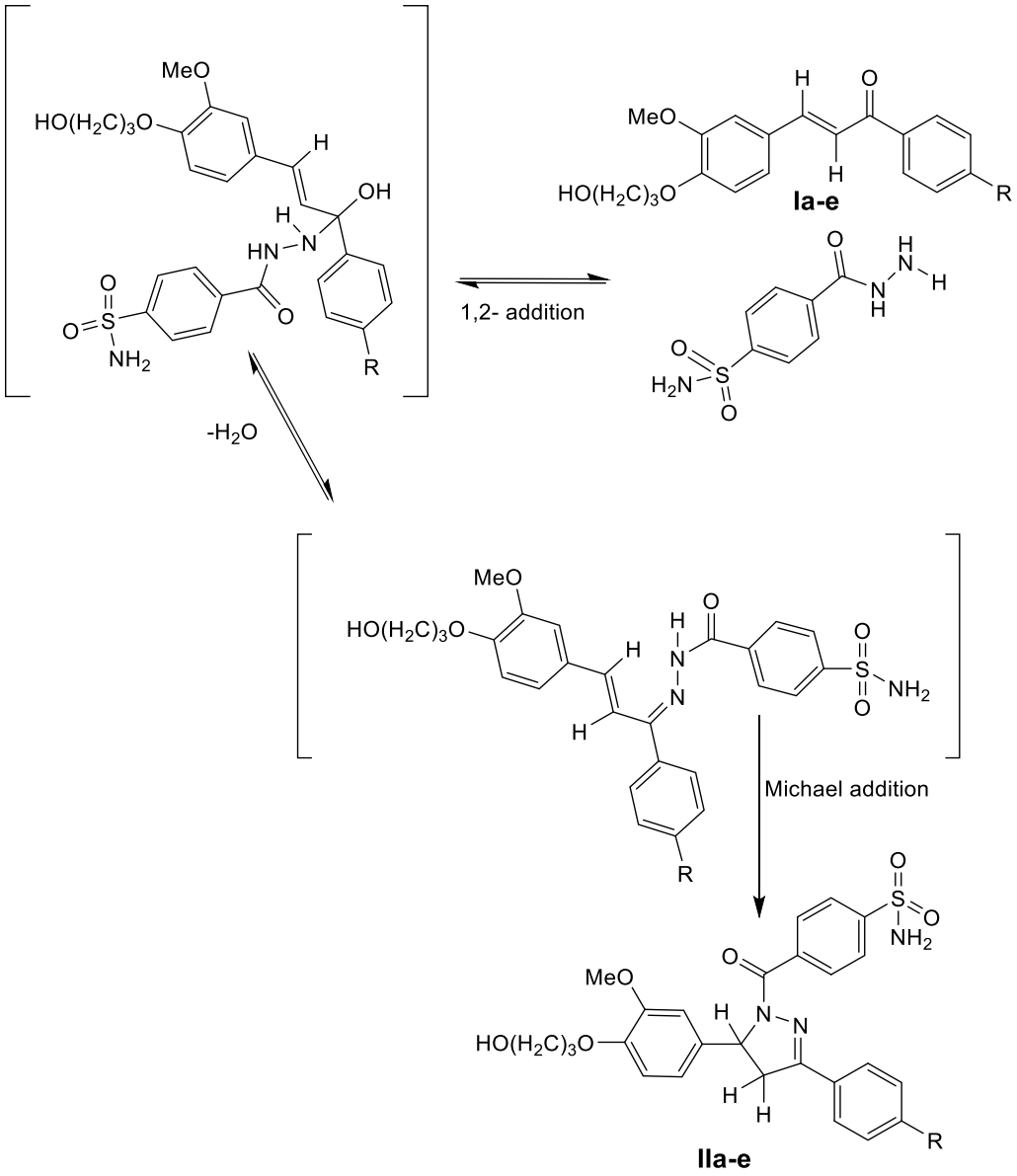

Scheme 2. The postulated mechanism for the formation of pyrazoline structures **IIa-e**

Pyrazoline-linked pyridine derivative **III** (Scheme 1) was obtained in good yield by treatment of **Ia** with isonicotinic acid hydrazide in glacial acetic acid. The synthesis of 1,5-thiazepine derivatives **IVa-e** was

achieved through treatment of chalcone derivatives with 2-aminothiophenol in the presence of conc. hydrochloric acid. This reaction begins with a nucleophilic addition, which is followed by a cyclisation and concomitant water elimination (Scheme 3).[23] The ^{1}H NMR spectrum revealed a characteristic peak at δ = 2.94-3.01 and δ = 3.51-3.56 ppm, which appeared as doublets of doublets integrated for methylene proton, while the C-H proton appeared around δ = 5.17-5.34 ppm as a doublet of doublets confirmed the product formed.

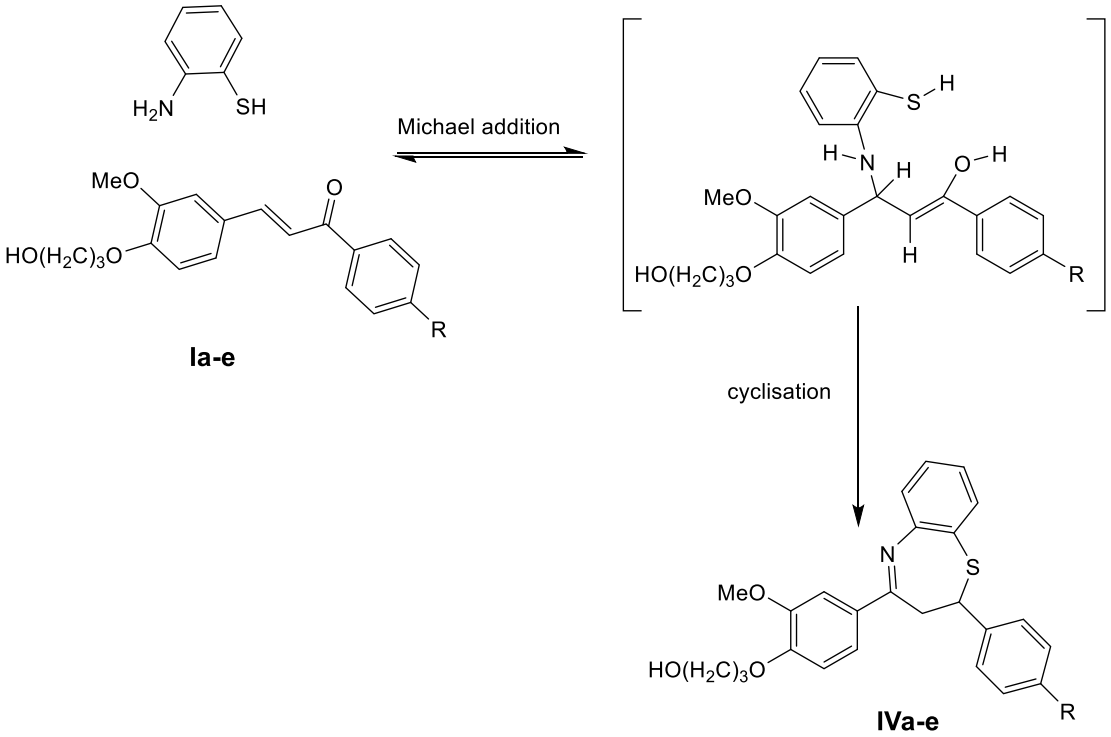

Scheme 3. The mechanism of the cycloaddition reaction leads to 1,5-benzothiazepines **IVa-e**

Biological Evaluation

In vitro cytotoxic activity

Some selected synthesised compounds were tested on a panel of four human cancer cell lines: HepG2 (liver), HEK-293 (kidney), MCF-7 (breast), and MDA-MB 231 (breast) using the MTT assay according to Mosmann,[24] where, 5-flurouracil was used as a reference drug. The results were presented as values for growth inhibitor concentration (IC_{50}) (Table 1). Some of the examined products had good to moderate inhibitory growth activity. Compounds **IIb**, and **IVe** were the most active variants against the HepG2 cell line, whereas compound **III** exhibited moderate activity against the MCF-7 cell line (Table1). Compound **IIb** demonstrated a better capacity to inhibit cell proliferation of liver-derived cell lines (HepG2), (IC_{50} = 4 ± 1 µg/mL).

Table 1. IC_{50} values of some new compounds against human cancer cell lines (μg/mL)

Compd. No.	HepG2	HEK-293	MCF-7	MDA-MB 231
Ia	6.1 ± 4	7.4 ± 1	9.1 ± 4	17.5 ± 1
Ib	8.4 ± 3	6.5 ± 1	9.6 ± 4	8.2 ± 2
Ie	4.8 ± 1	5.7 ± 6	11 ± 6	9.5 ± 3
IIa	6.1 ± 5	9.3 ± 6	10.1 ± 2	11.3 ± 6
IIb	4 ± 1	7.6 ± 2	21 ± 6	18.4 ± 3
IIe	5.4 ± 2	14.1 ± 3	9.2 ± 1	6.6 ± 4
III	8.1 ± 6	8.2 ± 4	5.5 ± 1	13.5 ± 1
IVa	5.2 ± 6	12.8 ± 1	8.5 ± 6	9.2 ± 5
IVb	6.4 ± 1	6 ± 1	18.4 ± 5	10.3 ± 2
IVe	4.7 ± 2	7.5 ± 3	20.4 ± 6	18.4 ± 3
5-FU	2.1 ± 0.5	3.4 ± 0.5	2.2 ± 0.5	2.5 ± 0.5

The Inhibitory Effect on Tubulin Polymerization

Antimitotic drugs are one of the most commonly utilised chemotherapeutic medications in the treatment of metastatic cancer types.[25] These drugs bind to tubulin, a key protein in the mitotic spindle, producing a reduction in the dynamics of microtubules in the mitotic spindles; inhibiting construction and disrupts sister chromatids' normal movement towards the spindle poles.[26]

Accordingly, the tubulin beta polymerization inhibitory effect of the target compound was assessed using colchicine as a reference drug in order to evaluate the role of tubulin beta polymerization (TUBβ) on HepG2 cell proliferation and to figure out the possible mode of the most selective cytotoxic compounds towards hepG2 cells. This assay was carried out on compounds **IIb** and **Ve** which showed the greatest potential against the HepG2 cell line. However, the inhibitory effect of the target compounds on TUBβ was determined and the IC_{50} values were derived as shown in Table 2.

Table 2. Tubulin polymerization inhibiting effect of the target compounds

compounds	IC_{50}
IIb	2.2±0.13
Ve	4.13±0.28
colchicine	6.91±0.24

The two studied compounds had strong TUBβ inhibitory activity, which matched their cytotoxic efficacy against the HepG2 cell line *in vitro*. Compound **IIb** showed a marked inhibitory effect with an IC_{50} value of 2.86 µM; about 2.5 times more active than colchicine. However, compound **Ve** showed moderate cytotoxic effect against HepG2.

Apoptotic character and cell cycle arrest

Comound **IIb** was chosen for further investigations of its cellular mechanism of action regarding its effect on cell cycle progression and its induction of apoptosis on HepG2 cancer cells.

The evaluation of the apoptosis process was carried out *via* flow cytometry using propidium iodide (PI) and annexine V-FITC on HepG2.[27]

The cells were labeled with two dyes after treatment with compound **IIb**, IC_{50} concentration (4 µg/mL) for 24 h. The corresponding red (PI) and green (FICT) fluorescence were detected with the flow cytometry, in comparison to DMSO as a negative control (Figure 3). Compound **IIb** induced an increase in late/secondary cellular apoptosis from 0.09% (DMSO control) to 9.63%. In addition, compound **IIb** caused a 5.44% increase in early/primary apoptosis (0.18% DMSO control). The apoptotic character of compound **IIb** was supported by these findings.

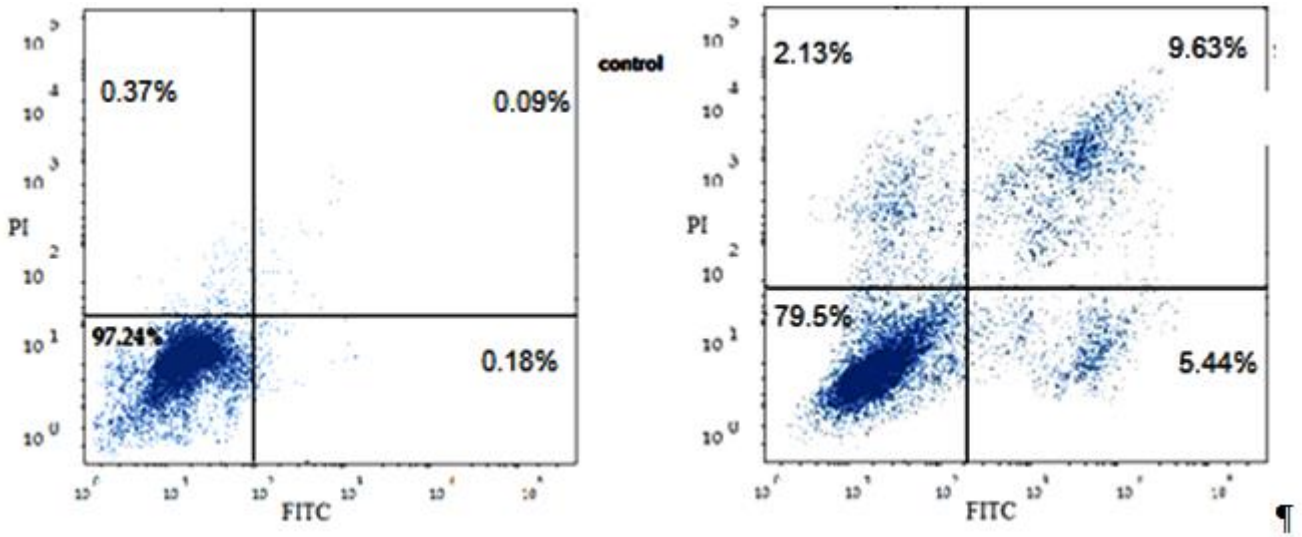

Figure 3. Compound **IIb**: Cellular mechanism of action. Induction of apoptosis by compound **IIb**. Cells were exposed to **IIb** for 24 h and analyzed by annexin V/PI staining. The percentage of cells undergoing apoptosis is defined as the sum of early apoptotic (annexin V+/PI-) cell percentage and late apoptotic (annexin V+/PI+) cell percentage.

Towards a better understanding of the cytotoxic mechanism of compound **IIb** against HepG2, flow cytometry was used to examine the anti-proliferative effect of the cell as well as its effect on cycle distribution. Compound **IIb** induced a significant increase in the percentage of cells in the pre-G1 phase

by 28.6 times more compared to control. However, cell accumulation was detected at G2/M phase, which was 5 times higher than in the control group, ranging from 8.59% in the vehicle group to 43.59% in the compound **IIb** group (Figure 4).

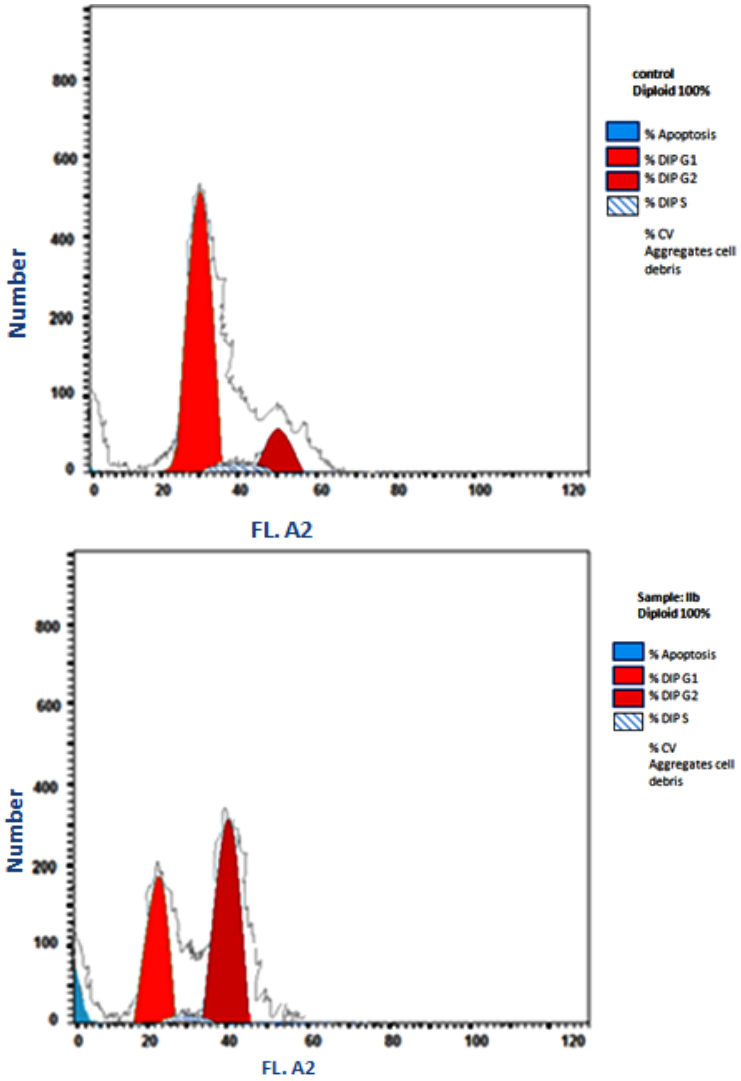

Figure 4. Cell cycle analysis of HepG2 after incubation with compound **IIb** for 24 h. DMSO was used as a control.

These results showed that compound **IIb** inhibited HepG2 cell proliferation through the induction of G2/M phase arrest, which led to cell cycle cessation, and prevented its mitotic cycle.

Effect of compound IIb on active caspas-7 (CASP-7)

Caspases are cestein protases, which play a fundamental role in apoptosis initiation due to pro-apoptotic signals. Therefore, activating caspases is a significant step in apoptotic cell death.[28]

CASP-7 levels were measured in HepG2 cells treated for 24 h with compound **IIb** at a concentration of 4 g/mL. They revealed a significant increase in CASP-7 levels compared to doxorubicin (Table 3).

Table 3. Caspase-7 concentration in HepG2 cells after treatment with compound **IIb** for 24 h

compound	Results		
	Conc. (µg/mL)	**CASP-7 conc. (µg/mL)**	**FLD (µg/mL)**
IIb	4.1	1.201	3.225769
doxorubicin	19.1	1.712	5.050128
control		0.348	1.00000

Microscopic Studies

Morphological changes in HepG2 cells after treatment with (4.0 µg) of compound **IIb** were studied for morphological variations using phase contrast microscopy. Changes in surface morphology were observed after 24 and 48 h (Figure 5).

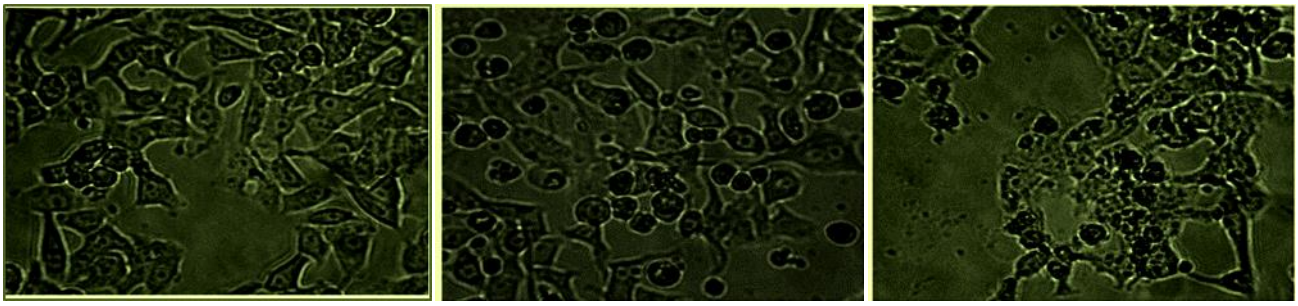

Figure 5. untreated control 24 h Exposure 48 h Exposure

After 24 h of exposure, the cells begin to exhibit apoptotic characteristics, in which the majority of the cells lose their normal branch-shaped appearance and shrinkage occurs. However, after 48 h of exposure, blabbing and lack of basal attachment as well as membrane asymmetry are markedly seen.

Docking Interpretation and Discussion

We identified the molecular binding mechanisms of tubulin bounded inside the pockets of the tested molecule with colchicine. The proposed molecular docking algorithm was first confirmed by re-docking the co-crystallized ligand into the active site of the corresponding receptor and calculating the root mean square deviation (RMSD) for reliability and repeatability. The RMSD 1.20 reached 2.00 Å, when docked on tubulin coupled with colchicine (PDB code: 1SA0), suggesting a validated algorithm when compared to the crystallographic structure.

The binding mode of the crystal ligand (colchicine) exhibited an energy binding of (-8.60 kcal mol^{-1}) against tubulin bounded with colchicin, Where the benzo[*a*]heptalene ring formed eight Pi-Alkyl interactions with *Leu248*, *Ala250*, *Ala316*, *Ala180*, and *Leu255*. Additionally, the carbonyl group

interacted with *Lys352* by one hydrogen bond with a distance of 1.60 Å, while the acetamide moiety formed one hydrogen bond with a distance of 1.88 Å with *Ser178*. (Figure 6).

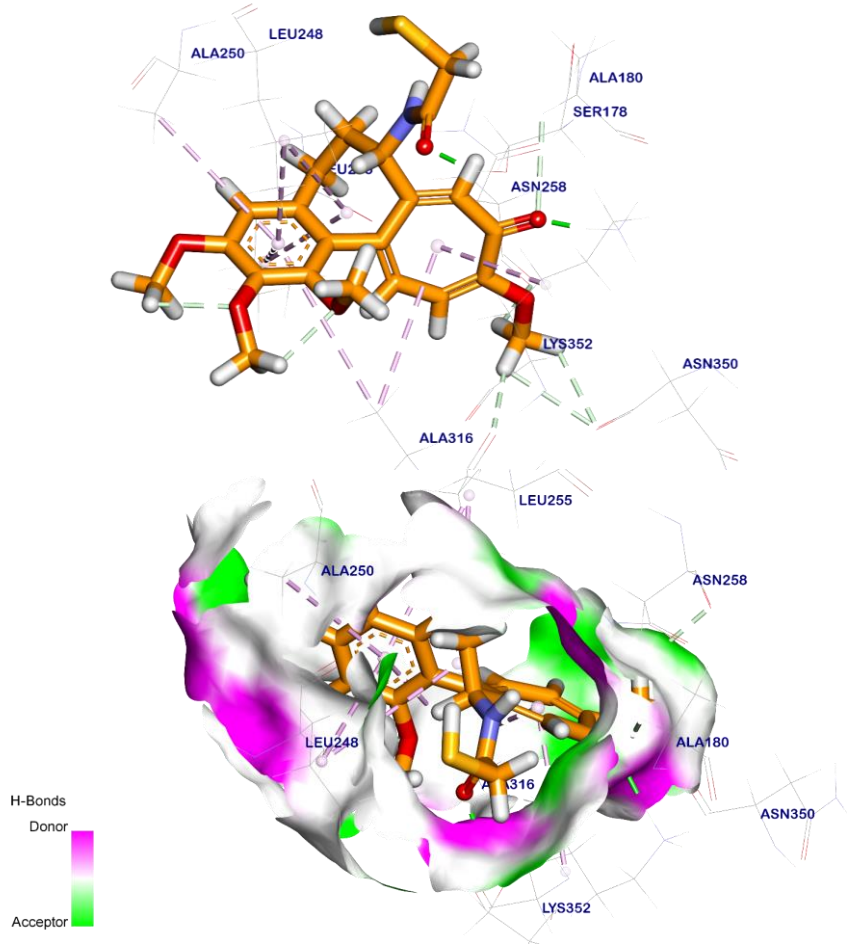

Figure 6. The crystal ligand (colchicine) docked in tubulin

Binding sites of the most biologically active cytotoxic candidate shown under here in Table 4 and Figures 7-9.

Table 4. (ΔG) kcal/mol of **IIb**, **III**, and **IVe** against tubulin bounded with colchicine target site (PDB code: 1SA0)

Ligand	Docking Score (Kcal/mol)	Interactions				RMSD (Å)
		H.B.	Binding mode	Pi-B.	Binding mode	
IIb	-10.33	4	2 (Gal11, Tyr224) 1 (Aln 250) 1 (Tyr202)	7	1 (Leu248) 1 (Asn258) 3 (Ly352, Ala316, Val182) 2 (Leu225, Ala250)	1.34

III	-8.26	1	Gln247	8	2 (Ala316, Lys352) 5 (Ala250, Cys241, Leu242, Leu255, Leu248) 1 (Leu248)	1.86
IVe	-9.69	4	3 (Leu248, Lys254, Thr179) 1 (Tyr202)	4	2 (Lys352, Ala316) 2 (Ala250, Leu255)	1.10

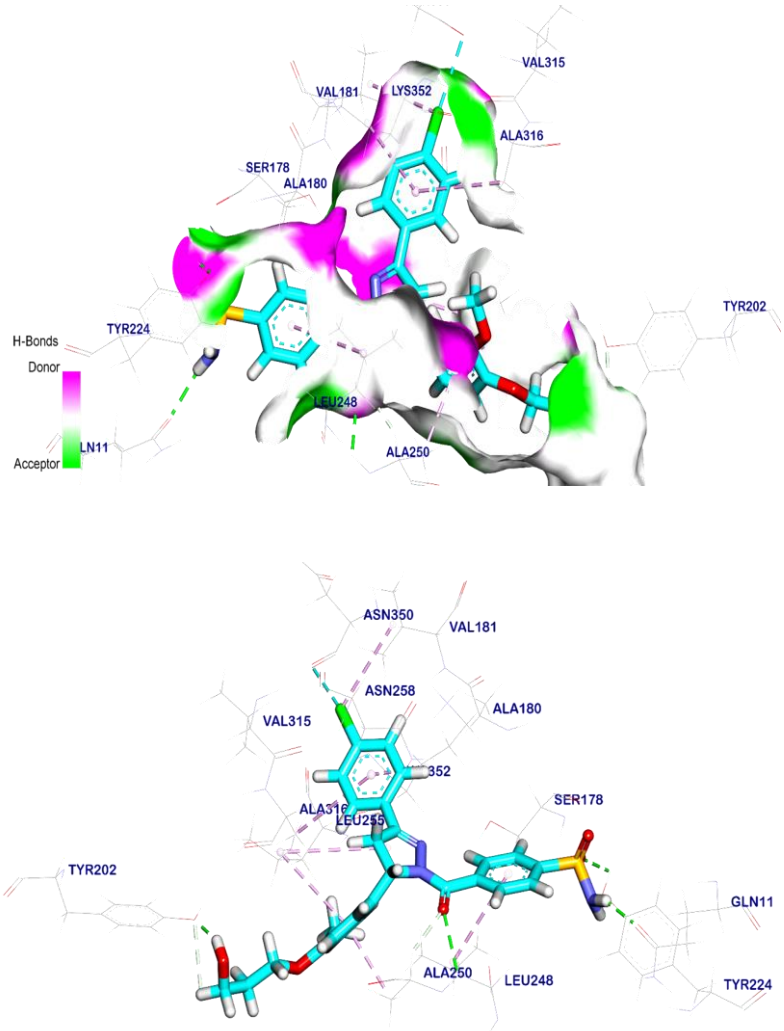

Figure 7. Compound **IIb** docked in tubulin bounded with colchicine, H.B. (green), the pi interactions (purple). Mapping surface showing compound **IIb** occupying the active pocket of tubulin bounded with colchicine.

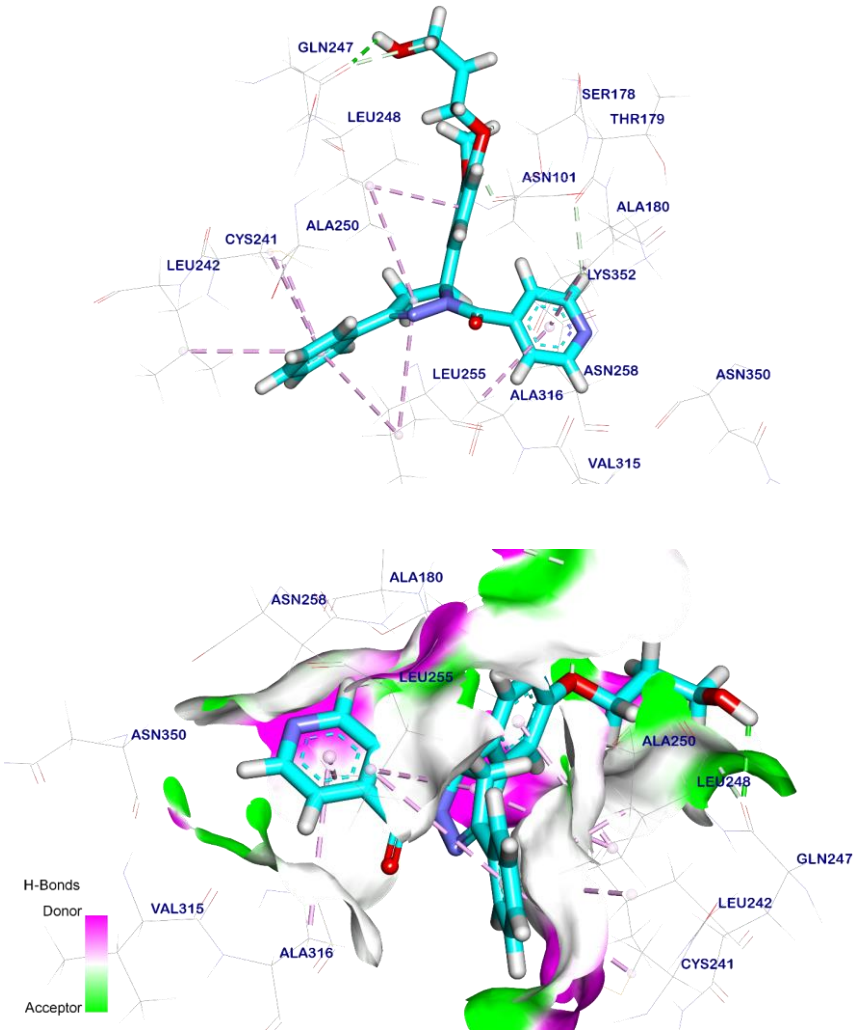

Figure 8. Compound **III** docked in tubulin bounded with colchicine, H.B. (green) and the pi interactions (purple). Mapping surface showing compound **III** occupying the active pocket of tubulin bounded with colchicine.

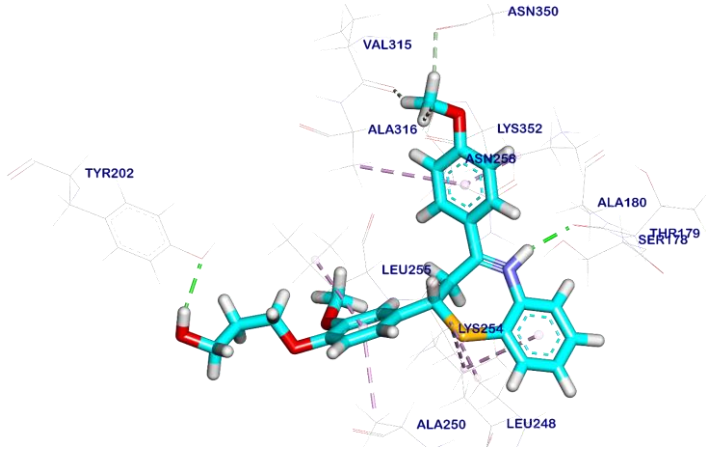

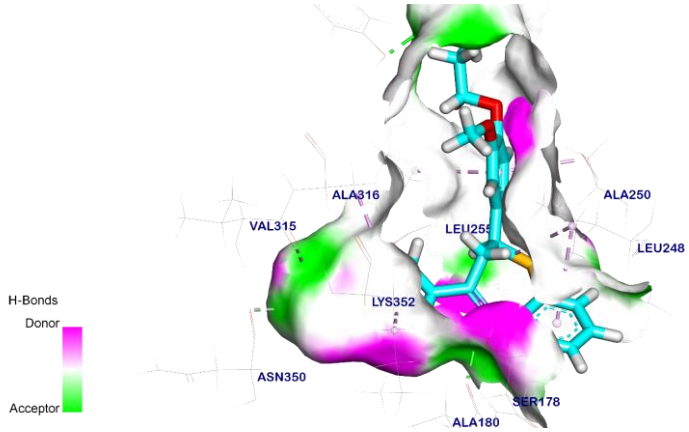

Figure 9. Compound **IVe** docked in tubulin bounded with colchicine, H.B. (green) and the pi interactions (purple). Mapping surface showing compound **IVe** occupying the active pocket of tubulin.

Pharmacophore profile prediction

Nguyen *et al.*,[29] discovered the common pharmacophore model of colchicine binding inhibitors, which consists of seven pharmacophore points: three H-bond acceptors, in contact with *Val181*, *Cys241*, and with *Ala250*, *Asp251*, and *Leu252*. hydrogen bond donor, interacts with *Thrb179*, two hydrophobic centers, and a planar group. It should be noted that none of the colchicine binding inhibitors possessed all seven pharmacophore points.[30]

Upon that, we predict the essential features of the pharmacophore profile of our tested compound by choosing the molecular targets that determine the main criteria's, hydrophobic moiety in U shape, linker and fragments containing hydrogen bond acceptors and donator to compare the compounds with crystal ligands and determine the essential features that can bind with critical amino acid at a target site. We used the ligand-based drug design (LBDD) protocol to compare the candidates with the crystal ligand as a reference for essential features (Table 5**)**.

Table 5. Matched essential features and pharmacophore fit score of **IIb**, **III**, **IVe** with the crystal ligand

Ligand	**Matching Features**	**No. of Essential features**	**Pharmacophore Fit score**
Pharmacophoric queries		5	-
IIb		3	54.93
III		3	52.90
IVe		3	51.31
colchicine		5	58.33

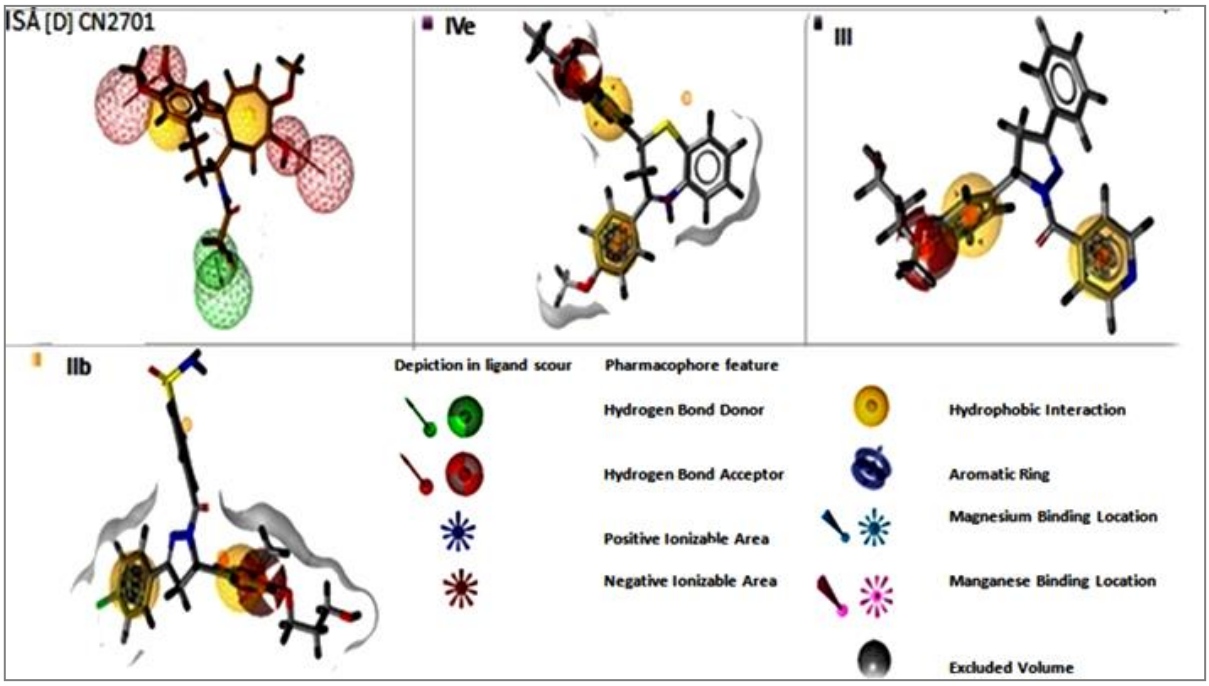

CONCLUSION

In conclusion, a class of novel pyrazolines and diaryl 1,5-benzothiazepine derivatives were synthesised from new chalcones and screened for their *in vitro* cytotoxic activity against HepG2, HEK-293, MCF-7, and MDA-MB-231 cancer cell lines, where, compound **IIb** showed the highest inhibition activity against HepG2 (liver cancer) cell lines with (IC_{50} = 4 ± 1 µg/mL). Consequently, compound **IIb**, showed marked suppression of tubulin polymerization compared to the reference drug. In addition, it induced cell cycle cessation at the G2/M phase, preventing its mitotic cycle. These results along with molecular docking analysis provide a trial of finding new cytotoxic agents targeting tubulin.

EXPERIMENTAL

Chemistry

Materials and Methods

All chemicals were provided by Aldrich companies and. Elemental microanalyses were carried out at Micro analytical Unit, Central Services Laboratory, National Research Centre, Dokki, Giza, Egypt, using Vario Elementary and were found within ± 0.4% of the theoretical values. All melting points were uncorrected and were taken in open capillary tubes using electro thermal apparatus 9100. FT-IR spectra were recorded with a Perkin-Elmer Frontier. Routine NMR spectra were recorded at room temperature on a Bruker Avance TM 500 MHz spectrometer as solutions in dimethyl sulfoxide (DMSO-d_6). All chemical shifts are quoted in δ relative to the trace resonance of protonated dimethyl sulfoxide (δ 2.50 ppm), DMSO (δ 39.51 ppm). The mass spectra were measured with a GC Finnegan MAT SSQ-7000 mass

spectrometer. The reactions were followed, and the purity of the compounds was checked using TLC on silica gel-percolated aluminum sheets (Type 60, F 254, Merck, and Darmstadt, Germany) and the spots were detected by exposure to UV lamp at λ254 nm. The chemical names given for the prepared compounds are according to the IUPAC system. The reported yields are based upon pure materials isolated. Solvents were dried/purified according to conventional procedures.

General procedure for the preparation of chalcones Ia-e.

To a solution of different substituted acetophenones (0.03 mol) and 4-(3-hydroxypropoxy)-3-methoxybenzaldehyde (0.03 mol) in EtOH was added ethanolic KOH (10%, 20 mL) under ice bath and stirred at rt for 6-10 h. The precipitated solid was filtered off, washed with cold water followed by EtOH and crystallized from MeOH.

(*E*)-3-[4-(3-Hydroxypropoxy)-3-methoxyphenyl]-1-phenyl-2-propen-1-one (Ia).

Yield 73%, mp 127-129 ºC; IR spectrum, ν, cm^{-1}: 3409 (OH), 1651 (CO); ^{1}H NMR spectrum, δ, ppm: 7.87 (d, 1H, *J* = 15.5 Hz, CH=CH-CO), 7.01-7.72 (m, 8H, ArH + CH=CH-CO), 4.12 (t, 2H, *J* = 6.4 Hz, CH_2), 3.96 (m, 2H, CH_2OH), 3.81 (s, 3H, OCH_3), 2.47 (br.s, 1H, OH), 2.09 (m, 2H, CH_2); ^{13}C NMR spectrum, δ, ppm: 189.51, 149.56, 146.12, 143.75, 138.02, 134.26, 129.68, 128.94, 127.83, 121.60, 119.28, 114.96, 111.34, 67.21, 60.82, 56.14, 31.84; MS: *m/z*: 312 $[M]^+$; Anal. Calcd for $C_{20}H_{22}O_5$, %: C, 73.06; H, 6.45. Found, %: C, 72.91; H, 6.52.

(*E*)-1-(4-Chlorophenyl)-3-[4-(3-hydroxypropoxy)-3-methoxyphenyl]-2-propen-1-one (Ib).

Yield 69%, mp 141-142 ºC; IR spectrum, ν, cm^{-1}: 3412 (OH), 1654 (CO); ^{1}H NMR spectrum, δ, ppm: 7.89 (d, 1H, *J* =15.5 Hz, CH=CH-CO), 6.95-7.70 (m, 8H, ArH + CH=CH-CO), 4.17 (t, 2H, *J* = 6.3 Hz, CH_2), 3.92 (m, 2H, CH_2), 3.79 (s, 3H, OCH_3), 2.49 (s, 1H, OH), 2.13 (m, 2H, CH_2); ^{13}C NMR spectrum, δ, ppm: 189.36, 149.77, 146.02, 143.27, 139.89, 135.97, 131.24, 129.36, 127.62, 123.18, 119.26, 114.99, 111.35, 64.82, 58.14, 56.22, 31.96; MS: *m/z*: 346 $[M]^+$; Anal. Calcd for $C_{19}H_{19}ClO_4$, %: C, 65.80; H, 5.52. Found, %: C, 65.62; H, 5.38.

(*E*)-1-(4-Bromophenyl)-3-[4-(3-hydroxypropoxy)-3-methoxyphenyl]-2-propen-1-one (Ic).

Yield 63%, mp 162-163 ºC; IR spectrum, ν, cm^{-1}: 3421 (OH), 1658 (CO); ^{1}H NMR spectrum, δ, ppm: 7.78 (d, 1H, *J* =15.5 Hz, CH=CH-CO), 7.05-7.71 (m, 8H, ArH + CH=CH-CO), 4.14 (t, 2H, *J* = 6.4 Hz, CH_2), 3.96 (m, 2H, CH_2), 3.82 (s, 3H, OCH_3), 2.51 (s, 1H, OH), 2.10 (m, 2H, CH_2); ^{13}C NMR spectrum, δ, ppm: 189.17, 149.86, 145.69, 143.78, 137.01, 132.16, 131.79, 128.59, 127.90, 121.76, 119.31, 115.26, 111.47, 64.76, 57.99, 56.37, 31.84; MS: *m/z*: 390 $[M]^+$; Anal. Calcd for $C_{19}H_{19}BrO_4$, %: C, 58.33; H, 4.89. Found, %: C, 58.16; H, 4.98.

(*E*)-3-[4-(3-Hydroxypropoxy)-3-methoxyphenyl]-1-(4-nitrophenyl)-2-propen-1-one (Id).

Yield 60%, mp 152-154 ºC; IR spectrum, ν, cm^{-1}: 3410 (OH), 1655 (CO); ^{1}H NMR spectrum, δ, ppm: 7.82 (d, 1H, *J* =15.5 Hz, CH=CH-CO), 7.01-7.72 (m, 8H, ArH + CH=CH-CO), 4.20 (t, 2H, *J* = 6.4 Hz,

CH_2), 3.90 (m, 2H, CH_2), 3.81 (s, 3H, OCH_3), 2.47 (s, 1H, OH), 2.12 (m, 2H, CH_2); ^{13}C NMR spectrum, δ, ppm: 189.76, 153.94, 149.71, 147.69, 144.13, 143.90, 131.06, 128.13, 122.09, 121.73, 119.47, 115.09, 110.96, 64.85, 58.19, 56.41, 32.01; MS: *m/z*: 357 $[M]^+$; Anal. Calcd for $C_{19}H_{19}NO_6$, %: C, 63.86; H, 5.36; N, 3.92. Found, %: C, 63.69; H, 5.47; N, 4.01.

(*E*)-3-[4-(3-Hydroxypropoxy)-3-methoxyphenyl]-1-(4-methoxyphenyl)-2-propen-1-one (Ie).

Yield 78%, mp 141-143 ºC; IR spectrum, ν, cm^{-1}: 3422 (OH), 1653 (CO); ^{1}H NMR spectrum, δ, ppm: 7.89 (d, 1H, *J* =15.5 Hz, CH=CH-CO), 7.01-7.74 (m, 8H, ArH + CH=CH-CO), 4.16 (t, 2H, *J* = 6.5 Hz, CH_2), 3.95 (m, 2H, CH_2), 3.78 (s, 3H, OCH_3), 2.53 (s, 1H, OH), 2.09 (m, 2H, CH_2); ^{13}C NMR spectrum, δ, ppm: 189.90, 165.91, 149.67, 145.12, 143.77, 131.01, 129.98, 128.02, 121.89, 119.27, 115.42, 114.78, 111.38, 65.04, 59.16, 56.63, 56.21, 31.85; MS: *m/z*: 342 $[M]^+$; Anal. Calcd for $C_{20}H_{22}O_5$, %: C, 70.16; H, 6.48. Found, %: C, 70.23; H, 6.29.

General procedure for the preparation of pyrazoline-linked benzenesulfonamides IIa-e from Ia-e.

A solution of the chalcones **Ia-e** (0.02 mol) and 4-(hydrazinecarbonyl)benzenesulfonamide (0.02 mol) was heated under reflux for 12 h in 20 mL of BuOH (monitored by TLC). The reaction mixture was left to cool, and the resulting solid was collected, dried, and recrystallized from MeOH.

4-(5-(4-(3-Hydroxypropoxy)-3-methoxyphenyl)-3-phenyl-4,5-dihydro-1*H*-pyrazole-1-carbonyl)-benzenesulfonamide (IIa).

Yield 64%, mp >300 ºC; IR spectrum, ν, cm^{-1}: 3418 (OH), 3310, 3251 (NH_2), 1680 (CO), 1186, 1148 (SO_2); ^{1}H NMR spectrum, δ, ppm: 8.14 (s, 2H, NH_2), 7.05-8.09 (m, 12H, ArH), 5.45 (dd, 1H, *J* = 17.6,4.7 Hz, CH), 4.19 (t, 2H, *J* = 6.6 Hz, OCH_2), 3.98 (m, 2H, CH_2OH), 3.79 (s, 3H, OCH_3), 3.74 (dd, 1H, *J* = 17.8, 11.7 Hz, CH_2 of pyrazoline), 3.21 (dd, 1H, *J* = 11.8, 4.8 Hz, CH_2), 2.51 (s, 1H, OH), 2.08 (m, 2H, CH_2); ^{13}C NMR spectrum, δ, ppm: 165.47, 153.28, 149.55, 147.65, 146.27, 139.86, 136.17, 132.98, 130.56, 129.06, 128.64, 127.92, 127.16, 119.25, 112.05, 110.31, 64.81, 62.16, 58.24, 56.19, 43.17, 31.79; MS: *m/z*: 509 $[M]^+$; Anal. Calcd for $C_{26}H_{27}N_3O_6S$, %: C, 61.28; H, 5.34; N, 8.25. Found, %: C, 61.39; H, 5.17; N, 8.09.

4-(3-(4-Chlorophenyl)-5-(4-(3-hydroxypropoxy)-3-methoxyphenyl)-4,5-dihydro-1*H*-pyrazole-1-carbonyl)benzenesulfonamide (IIb).

Yield 58%, mp >300 ºC; IR spectrum, ν, cm^{-1}: 3406 (OH), 3324, 3205 (NH_2), 1685 (CO), 1179, 1124 (SO_2); ^{1}H NMRspectrum, δ, ppm: 8.11 (s, 2H, NH_2), 7.01-8.09 (m, 11H, ArH), 5.47 (dd, 1H, *J* = 17.6, 4.6 Hz, CH), 4.18 (t, 2H, *J* = 6.4 Hz, CH_2), 3.94 (d, 2H, *J* = 6.2 Hz, CH_2), 3.91 (m, 2H, CH_2), 3.79 (s, 3H, OCH_3), 3.76 (dd, 1H, *J* = 17.8, 11.7 Hz, CH_2), 3.23 (dd, 1H, *J* = 11.8, 4.8 Hz, CH_2), 2.48 (s, 1H, OH), 2.12 (m, 2H, CH_2); ^{13}C NMR spectrum, δ, ppm: 165.71, 153.14, 149.37, 147.75, 147.05, 139.88, 137.02, 134.29, 133.49, 128.91, 128.16, 127.90, 126.31, 117.69, 111.96, 110.26, 64.52, 62.41, 58.74, 56.34, 43.09,

31.85; MS: *m/z*: 544 $[M]^+$; Anal. Calcd for $C_{26}H_{26}ClN_3O_6S$, %: C, 57.40; H, 4.82; N, 7.72. Found, %: C, 57.25; H, 4.96; N, 7.84.

4-(3-(4-Bromophenyl)-5-(4-(3-hydroxypropoxy)-3-methoxyphenyl)-4,5-dihydro-1*H*-pyrazole-1-carbonyl)benzenesulfonamide (IIc).

Yield 60%, mp >300 ºC; IR spectrum, ν, cm^{-1}: 3417 (OH), 3361, 3210 (NH_2), 1701 (CO), 1185, 1159 (SO_2). ^1H NMR spectrum, δ, ppm: 8.12 (s, 2H, NH_2), 7.01-8.10 (m, 11H, ArH), 5.52 (dd, 1H, *J* = 17.8, 4.9 Hz, CH), 4.16 (t, 2H, *J* = 6.6 Hz, CH_2), 3.93 (m, 2H, CH_2), 3.81 (s, 3H, OCH_3), 3.78 (dd, 1H, *J* = 17.8, 11.6 Hz, CH_2), 3.26 (dd, 1H, *J* = 11.7, 4.9 Hz, CH_2), 2.54(s, 1H, OH), 2.10 (m, 2H, CH_2); ^{13}C NMR spectrum, δ, ppm: 165.88, 152.10, 149.62, 148.37, 146.94, 141.01, 134.83, 132.98, 131.48, 128.55, 127.67, 127.35, 125.18, 117.79, 112.38, 110.46, 64.84, 62.34, 58.92, 56.24, 43.12, 31.74; MS: *m/z*: 588 $[M]^+$; Anal. Calcd for $C_{26}H_{26}BrN_3O_6S$, %: C, 53.07; H, 4.45; N, 7.14. Found, %: C, 52.90; H, 4.57; N, 7.21.

4-(5-(4-(3-Hydroxypropoxy)-3-methoxyphenyl)-3-(4-nitrophenyl)-4,5-dihydro-1*H*-pyrazole-1-carbonyl)benzenesulfonamide (IId).

Yield 52%, mp >300 ºC; IR spectrum, ν, cm^{-1}: 3414 (OH), 3319, 3215 (NH_2), 1690 (CO), 1187, 1134 (SO_2); ^{1}HNMR spectrum, δ, ppm: 8.11 (s, 2H, NH_2), 6.95-8.09 (m, 11H, ArH), 5.87 (dd, 1H, *J* = 17.9, 4.9 Hz, CH), 4.17 (t, 2H, *J* = 6.5 Hz, CH_2), 3.96 (m, 2H, CH_2), 3.81 (s, 3H, OCH_3), 3.79 (dd, 1H, *J* = 17.8, 11.6 Hz, CH_2), 3.39 (dd, 1H, *J* = 11.7, 4.9 Hz, CH_2), 2.46 (s, 1H, OH), 2.10 (m, 2H, CH_2); ^{13}C NMR spectrum, δ, ppm: 165.71, 151.24, 149.66, 148.96, 147.79, 146.82, 141.54, 138.97, 133.14, 128.04, 127.60, 127.19, 126.49, 118.10, 113.01, 110.59, 64.99, 62.04, 58.73, 56.37, 43.28, 31.68; MS: *m/z*: 554 $[M]^+$; Anal. Calcd for $C_{26}H_{26}N_4O_8S$, %: C, 56.31; H, 4.73; N, 10.10. Found, %: C, 56.14; H, 4.86; N, 9.91.

4-(5-(4-(3-Hydroxypropoxy)-3-methoxyphenyl)-3-(4-methoxyphenyl)-4,5-dihydro-1*H*-pyrazole-1-carbonyl)benzenesulfonamide (IIe).

Yield 65%, mp 298-300 ºC; IR spectrum, ν, cm^{-1}: 3420 (OH), 3313, 3206 (NH_2), 1689 (CO), 1180, 1137 (SO_2); ^1H NMR spectrum, δ, ppm: 8.14 (s, 2H, NH_2), 7.01-8.09 (m, 11H, ArH), 5.75 (dd, 1H, *J* = 17.8, 4.6 Hz, CH), 4.14 (t, 2H, *J* = 6.5 Hz, CH_2), 3.91 (m, 2H, CH_2), 3.79, 3.81 (2s, 6H, $2OCH_3$), 3.77 (dd, 1H, *J* = 17.8, 11.6 Hz, CH_2), 3.35 (dd, 1H, *J* = 11.7, 4.6 Hz, CH_2), 2.52 (s, 1H, OH), 2.11 (m, 2H, CH_2); ^{13}C NMR spectrum, δ, ppm: 164.79, 161.57, 151.48, 149.56, 148.23, 146.37, 138.91, 132.87, 128.65, 128.51, 127.76, 127.31, 119.02, 115.04, 112.92, 110.72, 64.82, 62.18, 58.29, 56.61, 56.25, 43.10, 31.46; MS: *m/z*: 539 $[M]^+$; Anal.Calcd for $C_{27}H_{29}N_3O_7S$, %: C, 60.10; H, 5.42; N, 7.79. Found, %: C, 59.92; H, 5.56; N, 7.63.

The Preparation of pyrazoline-linked pyridine III from Ia.

An equimolar quantities (0.001 mol) of chalcone (**Ia**) and isoniazid in glacial acetic acid (15 mL) were heated at 90 ºC for 12 h. The reaction mixture was cooled when the reaction was completed (TLC), poured onto ice-cold water, and neutralized with dil. ammonia soln. The separated solid was filtered, washed with water and recrystallized from MeOH.

[4,5-Dihydro-5-[4-(3-hydroxypropoxy)-3-methoxyphenyl)-3-phenyl]-1*H*-pyrazol-1-yl]-4-pyridinyl-methanone (III).

Yield 72%, mp 146-148 ºC; IR spectrum, ν, cm^{-1}: 3412 (OH), 1651 (CO); ^{1}HNMR spectrum, δ, ppm: 7.01-7.69 (m, 12H, ArH), 5.47 (dd, 1H, *J* = 17.7, 4.6 Hz, CH), 4.20 (t, 2H, *J* = 6.5 Hz, CH_2), 3.92 (m, 2H, CH_2), 3.79 (s, 3H, OCH_3), 3.98 (dd, 1H, *J* = 17.8, 11.7 Hz, CH_2), 3.41 (dd, 1H, *J* = 11.7, 4.8 Hz, CH_2), 2.49 (s, 1H, OH), 2.10 (m, 2H, CH_2); ^{13}C NMR spectrum, δ, ppm: 165.47, 151.64, 149.56, 148.92, 147.35, 141.02, 135.19, 132.40, 130.76, 128.69, 127.82, 121.48, 119.52, 113.41, 110.38, 68.14, 61.24, 58.94, 56.18, 42.62, 31.27; MS: *m/z*: 431 $[M]^+$; Anal. Calcd for $C_{25}H_{25}N_3O_4$, %: C, 69.59; H, 5.84; N, 9.74. Found, %: C, 69.41; H, 5.96; N, 9.57.

General procedure for the preparation of 1,5-benzothiazepines IVa-e from Ia-e

In hot EtOH, an equal equivalent (0.01 mol) of chalcone analogues **Ia-e** and 2-aminothiophenol were added, then concentrated hydrochloric acid was added dropwise and the reflux was continuing for 6 h. After cooling, the crude product was collected, filtered and crystallized from MeOH.

3-[4-(2,3-Dihydro-2-phenyl-1,5-benzothiazepin-4-yl)-2-methoxyphenoxy]-1-propanol (IVa)

Yield 63%, mp 148-151 ºC; IR spectrum, ν, cm^{-1}: 1596 (C=N); ^{1}H NMR spectrum, δ, ppm: 6.95-7.90 (m, 12H, ArH), 5.21 (dd, 1H, *J* = 12.3, 4.6 Hz, SCH), 4.17 (t, 2H, *J* = 6.5 Hz, CH_2), 3.90 (m, 2H, CH_2), 3.79 (s, 3H, OCH_3), 3.54 (dd, 1H, *J* = 13.0, 4.6 Hz, CH_2), 2.98 (dd, 1H, *J* = 13.1, 4.6 Hz, CH_2), 2.53 (s, 1H, OH), 2.12 (m, 2H, CH_2). ^{13}C NMR spectrum, δ, ppm: 168.73, 153.41, 150.23, 148.36, 137.49, 137.15, 135.80, 132.79, 130.93, 128.63, 127.58, 126.97, 124.82, 119.72, 117.01, 112.35, 110.03, 64.91, 60.87, 60.14, 58.73, 56.41, 31.25; MS: *m/z*: 419 $[M]^+$; Anal. Calcd for $C_{25}H_{25}NO_3S$, %: C, 71.57; H, 6.01; N, 3.34. Found, %: C, 71.39; H, 5.86; N, 3.47.

3-[4-(2-(4-Chlorophenyl)-2,3-dihydro-[1,5]benzothiazepin-4-yl)-2-methoxyphenoxy]-1-propanol (IVb).

Yield 59%, mp 162-164 ºC; IR spectrum, ν, cm^{-1}: 1602 (C=N); ^{1}H NMR spectrum, δ, ppm: 6.80-7.65 (m, 11H, ArH), 5.34 (dd, 1H, *J* = 12.4, 4.7 Hz, SCH), 4.19 (t, 2H, *J* = 6.6 Hz, CH_2), 3.95 (m, 2H, CH_2), 3.82 (s, 3H, OCH_3), 3.56 (dd, 1H, *J* = 12.8, 4.6 Hz, CH_2), 2.94 (dd, 1H, *J* = 13.2, 4.7 Hz, CH_2), 2.52 (s, 1H, OH), 2.09 (m, 2H, CH_2). ^{13}C NMR spectrum, δ, ppm: 167.25, 154.10, 148.76, 143.97, 135.77, 134.06, 132.81, 131.57, 130.24, 128.53, 127.92, 126.84, 126.14, 121.90, 118.68, 113. 78, 112.28, 64.98, 61.09,

59.86, 58.79, 56.38, 31.46; MS: *m/z*: 453 $[M]^+$; Anal. Calcd for $C_{25}H_{24}ClNO_3S$, %: C, 66.14; H, 5.33; N, 3.09. Found, %: C, 66.23; H, 5.16; N, 3.26.

3-[4-(2-(4-Bromophenyl)-2,3-dihydro-[1,5]benzothiazepin-4-yl)-2-methoxyphenoxy]-1-propanol (IVc).

Yield 51%, mp 156-158 ºC; IR spectrum, ν, cm^{-1}: 1595 (C=N); ^{1}H NMR spectrum, δ, ppm: 6.85-7.65 (m, 11H, ArH), 5.17 (dd, 1H, *J* = 12.5, 4.7 Hz, SCH), 4.12 (t, 2H, *J* = 6.7 Hz, CH_2), 3.94 (m, 2H, CH_2), 3.80 (s, 3H, OCH_3), 3.51 (dd, 1H, *J* = 13.0, 4.5 Hz, CH_2), 2.96 (dd, 1H, *J* = 13.1, 4.7 Hz, CH_2), 2.49 (s, 1H, OH), 2.12 (m, 2H, CH_2); ^{13}C NMR spectrum, δ, ppm: 167.09, 154.36, 149.70, 144.21, 134.06, 133.41, 132.59, 131.45, 130.72, 127.99, 127.16, 126.38, 124.85, 121.93, 119.56, 114.91, 112.26, 65.04, 61.13, 59.78, 58.69, 56.22, 31.19; MS: *m/z*: 498 $[M]^+$; Anal. Calcd for $C_{25}H_{24}BrNO_3S$, %: C, 60.24; H, 4.85; N, 2.81. Found, %: C, 60.12; H, 4.67; N, 2.94.

3-[2-Methoxy-4-(2-(4-nitrophenyl)-2,3-dihydro-[1,5]benzothiazepin-4-yl)phenoxy]-1-propanol (IVd).

Yield 55%, mp 181-183 ºC; IR spectrum, ν, cm^{-1}: 1594 (C=N); ^{1}H NMR spectrum, δ, ppm: 6.72-7.90 (m, 11H, ArH), 5.31 (dd, 1H, *J* = 12.6, 4.6 Hz, SCH), 4.16 (t, 2H, *J* = 6.6 Hz, CH_2), 3.97 (m, 2H, CH_2), 3.82 (s, 3H, OCH_3), 3.52 (dd, 1H, *J* = 13.0, 4.5 Hz, CH_2), 3.01 (dd, 1H, *J* = 13.2, 4.7 Hz, CH_2), 2.51 (s, 1H, OH), 2.10 (m, 2H, CH_2); ^{13}C NMR spectrum, δ, ppm: 166.73, 154.90, 151.04, 148.81, 143.75, 138.97, 134.12, 132.52, 129.65, 127.86, 126.79, 126.19, 121.95, 121.03, 120.47, 115.10, 111.89, 64.91, 61.08, 60.14, 58.39, 56.18, 31.26; MS: *m/z*: 464 $[M]^+$; Anal. Calcd for $C_{25}H_{24}N_2O_5S$, %: C, 64.64; H, 5.21; N, 6.03. found, %: C, 64.49; H, 5.31; N, 5.86.

3-[2-Methoxy-4-(2-(4-methoxyphenyl)-2,3-dihydro-[1,5]benzothiazepin-4-yl)phenoxy]-1-propanol (IVe).

Yield 61%, mp 170-172 ºC; IR spectrum, ν, cm^{-1}: 1598 (C=N); ^{1}H NMR spectrum, δ, ppm: 6.70-7.82 (m, 11H, ArH), 5.20 (dd, 1H, *J* = 12.6, 4.7 Hz, SCH), 4.17 (t, 2H, *J* = 6.7 Hz, CH_2), 3.92 (m, 2H, CH_2), 3.81 (s, 3H, CH_3), 3.78 (s, 3H, OCH_3), 3.52 (dd, 1H, *J* = 13.1, 4.6 Hz, CH_2), 2.97 (dd, 1H, *J* = 13.1, 4.7 Hz, CH_2), 2.53 (s, 1H, OH), 2.09 (m, 2H, CH_2); ^{13}C NMR spectrum, δ, ppm: 167.17, 163.01, 154.87, 149.61, 143.90, 133.89, 132.73, 130.16, 128.02, 127.34, 126.37, 124.95, 121.76, 119.61, 114.89, 113.78, 110.93, 64.97, 60.83, 60.01, 59.21, 56.17, 55.76, 31.45; MS: *m/z*: 449$[M]^+$; Anal. Calcd for $C_{26}H_{27}NO_4S$, %: C, 69.46; H, 6.05; N, 3.12. Found, %: C, 69.27; H, 5.89; N, 3.23.

Biological Studies

Materials and Methods

Human cancer cell lines: HepG2 (Liver), HEK-293 (Kidney), MCF-7(Breast), and MDA-MB-231 (Breast) were grown in DMEM media supplemented with 10% bovine serum, 1X penicillin-streptomycin

(Sigma-Aldrich) at 37 ºC in a humidified chamber with 5% CO_2. 5-Flurouracil (sigma) was used as the reference drug (standard).

Treatment

Cells were seeded (1X105 cells/well in triplicate) in a 96-well flat-bottom plate (Becton-Dickinson Lab ware) a day before treatment and grown. Stocks of all extracts/compound (1.0 mg/mL) were made with 5% DMSO (Sigma-Aldrich) and further working solutions (100 µg/mL) were prepared in serum-free culture media. Cells were treated with four different doses (2, 6.2, 12.5, and 25 µg/mL; in triplicate) of the compounds, in complete growth media, including reference drug, was further incubated for 48 h.

Cell Proliferation and Viability Assay

On day 2 of treatment, cell proliferation and viability test was performed using TACS MTT Cell Proliferation and Viability Assay Kit (TACS) as per manufacturer's instructions. The response parameter calculated was the IC_{50} value, which corresponds to the concentration required for 50% inhibition of cell viability.

IC_{50} Determination

IC_{50} values were calculated for the promising active compounds possessing ≥ 70% cytotoxicity. Probit analysis was utilized assessed by the SPSS computer program (version 9/ 1989 SPSS Inc., USA).

Enzyme-linked assay for tubulin beta (TUBβ)

DMEM (supplemented with 10% FBS and 1% penicillin-streptomycin. Plate cells (cells density 1.2 – 1.8 × 10,000 cells/well) in a volume of 100 µL complete growth medium and 100 µL of the tested compound per well in a 96-well plate were used to cultured HepG2 cells for 20–24 h before the enzyme assay for tubulin. This kit includes a microtiter plate that has been pre-coated with a TUBβ-specific antibody. Samples are then added to the suitable microtiter plate wells with a biotin-conjugated antibody specific to TUBβ. Next, Avidin conjugated to horseradish peroxidase (HRP) is added to each microplate well and incubated. After TMB substrate solution is added, only those wells that contain TUBβ, biotin- conjugated antibody and enzyme-conjugated avidin will exhibit a change in color. The enzyme- substrate reaction is terminated by the addition of sulphuric acid solution and the color change is measured spectrophotometrically at a wavelength of 450 nm ± 10 nm. By comparing the O.D. of the samples to the standard curve, the concentration of TUBβ in the samples is determined.[31]

Cell cycle analysis

Apoptotic character and cell cycle analysis were carried out by flow cytometry. HepG2 cells were seeded at 8×104 and incubated at 37 ºC, 5% CO_2 overnight. Tested compound **IIb**, was treated for 24 h, cell pellets were collected and centrifuged (300×g/5 min) for cell cycle analysis, cell pellets were fixed with 70% EtOH on ice for 15 min and collected again.[27] The collected pellets were incubated with propidium

iodide (PI) staining solution at room temperature for 1 h. Apoptosis detection was performed by Annexin V-FITC apoptosis detection kit (BioVision, Inc, Milpitas, CA, USA) following the manufacturer's protocol. The samples were analyzed using flow cytometer (BD Biosciences, San Jose, CA).

Caspase-7 assay

Caspase-7 were activated and measured using Human CASP7 (Caspase 7) ELISA Kit (My Bio-Source, Inc., San Diego, CA, USA) according to the manufacturer instructions.

Microscopy Studies

The cells were seeded in 6-well plates and allowed to adhere at 37 ^{o}C in CO_2 incubator. After 24 h, each well was treated with 10 μg of target compound and incubated for the indicated time. After 24 and 48 h, the cells were imaged by phase contrast microscope (Olympus CLX 41) to visualize morphological changes in HepG2 cells.

Docking Study

Using MOE 19.0901 Software, after doing a pharmacophore analysis and picking the protein of the target site, several operations were carried out to provide understanding of the molecular binding mechanisms of the investigated drugs within the pockets of tubulin bound with colchicine. The co-crystallized ligand has been used to create the binding sites inside the crystal protein (PDB code: 1SA0). Chem-Bio Draw Ultra17.0 was used to create 2D structures of the chemicals studied, which were then stored in MDL-SD format. The energy of 3D structures was reduced by using a 0.05 RMSD kcal/mol MMFF94 force field. Then, following the prepares ligand protocol, the minimized structures were prepared for docking.[32] The CDOCKER protocol was used to carry out the molecular docking procedure. During the refinement, the receptor was kept inflexible while the ligands were permitted to be flexible. Each molecule was given ten possible interaction postures with the protein. Then, using Discovery Studio 2019 Client software, docking scores of the best-fitted postures with the active site at (tubulin bounded by colchicine) were recorded, and a 3D view was produced. Re-docking of the co-crystallized ligand into the active site of the corresponding receptor with the calculation of root mean square deviation (RMSD) for reliability and repeatability of the proposed docking technique has been used to validate the molecular docking technique. The RMSD 1.20 blew 2.00 Å when docked on tubulin coupled with colchicine (1SA0), demonstrating a validated algorithm when compared to the crystallographic structure.

COMPLIANCE WITH ETHICAL STANDARDS

No animals were involved in this work. No human subjects were involved in this work.

CONFLICT OF INTEREST

The authors declared no conflict of interest.

REFERENCES

1. C. To, J. B. Jang, T. Chen, E. Park, M. Shajiang, D. J. H. DeClercq, M. Xu, S. Wang, M. D. Cameron, D. E. Heppner, B. H. Shin, T. W. Gero, A. N. Yang, S. E. Dahlberg, K. K. Wong, M. J. Eck, N. S. Gray, and P. A. Janne, *Cancer Discov.*, 2019, **9**, 926.
2. C. H. Liu, D. D. Wang, S. Y. Zhang, Y. R. Cheng, F. Yang, Y. Xing, T. L. Xu, H. F. Dong, and X. J. Zhang, *ACS Nano*, 2019, **13**, 4267.
3. W. P. Zou, J. D. Wolchok, and L. P. Chen, *Sci. Transl. Med.*, 2016, **8**, 328.
4. Y. X. Wang, H. Zhang, B. Gigant, Y. M. Yu, Y. P. Wu, X. Z. Chen, Q. H. Lai, Z. Y. Yang, Q. Chen, and J. L. Yang, *FEBS J.*, 2016, **283**, 102.
5. M. K. Gardner, M. Zanic, and J. Howard, *Curr. Opin. Cell Biol.*, 2013, **25**, 14.
6. J. Liu, C. H. Zheng, X. H. Ren, F. Zhou, W. Li, J. Zhu, J. G. Lv, and Y. J. Zhou, *J. Med. Chem.*, 2012, **55**, 5720.
7. C. Dumontet and M. A. Jordan, *Nat. Rev. Drug Discov.*, 2010, **9**, 790.
8. Z. S. Bai, M. O. Gao, and H. Z. Zhang, *Cancer Lett.*, 2017, **402**, 81.
9. M. Cornago, C. Garcia-Alberich, N. Blasco-Angulo, N. Vall-Ilaura, and M. Nager, *Cell Death Dis.*, 2014, **5**, 1435.
10. R. Kaur, G. Kaur, R. K. Gill, R. Soni, and J. Bariwal, *Eur. J. Med. Chem.*, 2014, **87**, 89.
11. D. Simoni, R. Romagnoli, R. Baruchello, R. Rondanin, M. Rizzi, M. G. Pavani, D. Alloatti, G. Giannini, M. Marcellini, T. Riccioni, M. Castorina, M. B. Guglielmi, F. Bucci, P. Carminati, and C. Pisano, *J. Med. Chem.*, 2006, **49**, 3143.
12. Y. T. Ji, Y. N. Liu, and Z. P. Liu, *Curr. Med. Chem.*, 2015, **22**, 1348.
13. P. D. Davis, G. J. Dougherty, D. C. Blakey, S. M. Galbraith, G. M. Tozer, A. L. Holder, M. A. Naylor, J. Nolan, M. R. L. Stratford, D. J. Chaplin, and S. A. Hill, *Cancer Res.*, 2002, **62**, 7247.
14. P. Zhou, Y. Liu, L. Zhou, K. Zhu, K. Feng, H. Zhang, Y. Liang, H. Jiang, C. Luo, M. Liu, and Y. Wang, *J. Med. Chem.*, 2016, **59**, 10329.
15. D. V. Tsyganov, L. D. Konyushkin, I. B. Karmanova, S. I. Firgang, Y. A. Strelenko, M. N. Semenova, A. S. Kiselyov, and V. V. Semenov, *J. Nat. Prod.*, 2013, **76**, 1485.
16. Q. Li, X. E. Jian, Z. R. Chen, L. Chen, X. S. Huo, Z. H. Li, W. W. You, J. J. Rao, and P. L. Zhao, *Bioorg. Chem.*, 2020, **201**, 104076.
17. N. Khalifa, N. Ismail, and M. Abdulla, *Egyptian Pharm. J.*, 2005, **4**, 277.
18. N. Khalifa, A. Adel, S. Abd-Elmoez, O. Fathalla, and A. Abd El-Gwaad, *Res. Chem. Intermed.*, 2015, **41**, 2295.
19. M. E. Haiba, E. S. Al-Abdullah, M. M. Edrees, and N. M. Khalifa, *Drug Res.*, 2015, **65**, 917.
20. N. M. Khalifa, M. S. Mohamed, M. E. Zaki, M. A. Al-Omar, and Y. M. Zohny, *Res. Chem.*

Intermed., 2014, **40**, 1565.

21. N. M. Khalifa, M. A .Al-Omar, A. E. Amr, A. R. Baiuomy, and R. F. Abdel-Rahman, *Russ. J. Bioorg. Chem*., 2015, **41**, 192.
22. A. Hoz, I. Alkorta, and J. Elguero, *Tetrahedron*, 2021, **97**, 132413.
23. B. C. Sekhar, *Acta Chim. Slov*., 2014, **61**, 651.
24. T. Mosmann, *J. Immunol. Methods*, 1983, **65**, 55.
25. N. G. Davidson, *Semin. Oncol*., 1995, **22**, 2.
26. M. A. Jordan, D. Thrower, and L. Wilson, *Cancer Res.*, 1991, **51**, 2212.
27. S. Diab, T. Teo, M. Kumarasiri, P. Li, M. Yu, F. Lam, S. K. Basnet, M. J. Sykes, H. Albrecht, and R. Milne, *ChemMedChem*, 2014, **9**, 962.
28. J. Li and J. Yuan, *Oncogene*, 2008, **27**, 6194.
29. T. L. Nguyen, C. A. McGrath, R. Hermone, J. C. Burnett, D. W. Zaharevitz, B. W. Day, and P. Wipf, *J. Med. Chem*., 2005, **48**, 6107.
30. X. Zhang, Y. Kong, J. Zhang, M. Su, Y. Zhou, Y. Zang, J. Li, Y. Chen, Y. Fang, and W. Lu, *Eur. J. Med. Chem*., 2015, **95**, 127.
31. K. Liliom, A. Lehotzky, A. Molnár, and J. Ovádi, *Anal. Biochem*., 1995, **228**, 18.
32. B. B. Jitender, D. U. Kuldip, T. M. Atul, C. T. Jalpa, S. S. Jyoti, S. J. Kishor, and K. S. Anamik, *Eur. J. Med. Chem*., 2008, **43**, 2279.